

Asymmetries in the electron-hole pair dynamics and strong Mott pseudogap effect in the phase diagram of cuprates

M.Z. Hasan,^{1,2,*} Y. Li,¹ D. Qian,¹ Y.-D. Chuang,³ H. Eisaki,⁴ S. Uchida,⁵ Y. Kaga,⁶ T. Sasagawa,⁶ and H. Takagi^{4,6}

¹*Department of Physics, Joseph Henry Laboratories, Princeton University, Princeton, NJ 08544*

²*CMC-CAT, Advanced Photon Source, Argonne National Laboratory, Argonne, IL 08544*

³*Advanced Light Source, Lawrence Berkeley National Lab, Berkeley, Ca 94720*

⁴*AIST, 1-1-1 Central 2, Umezono, Tsukuba, Ibaraki, 305-8568 Japan*

⁵*Department of Physics, University of Tokyo, Tokyo 113-8656, Japan*

⁶*Department of Adv. Materials Science, University of Tokyo, Kashiwanoha, Chiba 277-8561, Japan and CREST-JST, Kawaguchi, Saitama 332-0012, Japan*

(Dated: April 20, 2017)

Electron behavior in doped Mott systems continues to be a major unsolved problem in quantum many-electron physics. A central issue in understanding the universal Mott behavior in a variety of complex systems is to understand the nature of their electron-hole pair excitation modes. Using high resolution resonant inelastic x-ray scattering (RIXS) we resolve the momentum dependence of electron-hole pair excitations in two major classes of doped copper oxides which reveals a Mott pseudogap over the full Brillouin zone and over the entire phase diagram. The pair bandwidth and zone-boundary pair velocity renormalize on either sides of the phase diagram at very different rates indicating strong particle-hole doping asymmetries observed for the first time.

PACS numbers: 78.70.Ck, 71.20.b, 74.25.Jb

The discovery of high temperature superconductivity, colossal magnetoresistance and other unusual electron transport behavior has led to extensive research interests in doped Mott insulators[1]-[7]. The unusual behavior of these systems are often described by charge transport, optical excitation spectrum or thermal and magnetic susceptibility measurements which essentially probe the density of electron-hole pair excitation modes, electronic charge or spin density of states. Transport or thermodynamic measurements do not resolve the momentum quantum numbers of pair excitations. Optical techniques which are typically used to study the electronic excitation spectrum and charge gap (Mott gap), are only confined near the zero momentum transfer due to the large wavelength compared to the lattice parameters[8, 9]. Resolving the pair excitations along the momentum axis provides a new and important dimension of information to understand the electron dynamics in complex systems.

A parent Mott insulator can be doped either with electrons or holes, and many physical properties such as transport and magnetism are very sensitive to the doping level. Understanding the doping evolution of the electronic structure in both dopant-sides is quite important. Electronic structure of cuprates has been extensively studied by Angle-resolved Photoemission spectroscopy (ARPES). However, ARPES provides key insights into the single particle dynamics only. Using high resolution resonant inelastic x-ray scattering [10, 11] we resolve the momentum dependence of electron-hole pair excitations in two major classes of copper oxide series including $\text{Nd}_{2-x}\text{Ce}_x\text{CuO}_4$ and $\text{La}_{2-x}\text{Sr}_x\text{CuO}_4$, systematically over the phase diagram to gain insights into the universal aspects of correlated electron motion in these

systems.

The inelastic x-ray scattering data were obtained at the CMC-CAT beamline 9-ID and BESSRC-CAT beamline 12-ID at the Advanced Photon Source, Argonne National Laboratory. The incident beam energy was selected near the copper K edge to produce enhancement of inelastic signals. The scattered beam was reflected off of a germanium (733) crystal analyzer and measured with a solid-state detector. The overall energy resolution for the experiment was 370 meV and all the data were taken at room temperature. Experimental details of scattering parameters are described in ref. [12,13]. Incident x-ray polarization was along the c -axis of all samples in a vertical scattering geometry. Furthermore, scattering was also performed in the horizontal geometry where the polarization was within the ab -plane to check for matrix element effects possibly suppressing intensity near the leading-edge of the gap. Data were taken with closely spaced momentum intervals in between $\mathbf{q} \sim \pi$ to 2π (\mathbf{q} being the scattering wave vector) to allow for leading-edge mid-point analysis of the gap for the first time.

Fig.1(top) shows pseudo-color plots of momentum-resolved charge excitation spectra in the electron-doped cuprate series $\text{Nd}_{2-x}\text{Ce}_x\text{CuO}_4$ (e-doped, $x=0.10, 0.13$) (a), hole doped cuprate series $\text{La}_{2-x}\text{Sr}_x\text{CuO}_4$ (h-doped, $x=0.02, 0.14$) (b) and undoped cuprate ($x=0$) (c) as a function of hole and electron doping (x) level. Quasielastic scattering was removed by fitting below 0.8 eV. A broad excitation band (cyan) is seen from 0.5 to 3 eV for the e-doped systems whereas the analogous excitations in the h-doped systems (red) appear in 2 to 5 eV energy range. These excitations are seen over the range of momentum transfers covering the full Brillouin zone.

Fig.1(d) is typical plot for momentum-resolved energy-loss spectra corresponding to the image in Fig.1(a)/left. Fig.1(e) shows selected energy-loss spectra near high

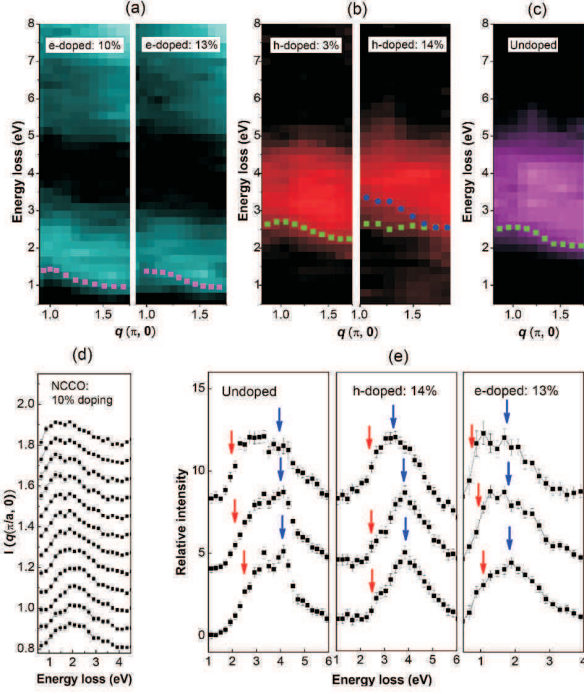


FIG. 1: Momentum-Resolved Charge Excitations in Cuprates: Momentum ($\hbar q$)-dependence of charge excitations in electron-doped $\text{Nd}_{2-x}\text{Ce}_x\text{CuO}_4$ (a), hole-doped $\text{La}_{2-x}\text{Sr}_x\text{CuO}_4$ (b) and undoped insulator (c) copper oxides. Brighter color indicates higher intensity. Dotted lines indicate the location of the leading edge of the gap except in case of LSCO ($x=0.14$) where a second dotted line traces out the second peak. (d) plots the q -resolved energy-loss spectra corresponding to the image plot (a)/left. (e) shows selected energy-loss curves near high symmetry points of the Brillouin zone for undoped, h -doped, and e -doped samples

symmetry points of the Brillouin zone to compare the effect of hole and electron doping by comparing insulator vs. metal. The lower energy edge (dotted lines in Fig.1(top)) of the dominant excitation defines the edge of the insulating charge gap (effective Mott gap) [in the insulator (Fig.1c)]. For the undoped sample (Fig.1c), near the zone center the onset of excitation edge is at the lowest in energy at about 1.8 eV, consistent with optical studies [8] where as the analogous excitation in NCCO series appears at around 1 eV, again consistent with optical studies [9]. The **leading-edge** mid-point of the gap observed here hardly disperses in going from the zone center ($q \sim 2\pi$) to $q \sim 1.4\pi$ (unlike earlier reports on La_2CuO_4 [14, 15] and a concurrent work on LSCO [16]). However, this behavior we observe is consistent with dispersions seen in other cuprates such as $\text{Ca}_2\text{CuO}_2\text{Cl}_2$ [12] and $\text{Sr}_2\text{CuO}_2\text{Cl}_2$ [14] and the $\text{Nd}_{2-x}\text{Ce}_x\text{CuO}_4$ series studied here.

With increased doping the spectra change in two major ways - a low-energy continuum appears below the gap as seen in Fig.2 and the momentum dependence of the leading edge weakens. A closer look in Fig.2 shows that the low-energy spectral weight grows (reddish/bluish continuum in Fig.1a and Fig.1b) at the expense of the spectral weight around 2 to 3.5 eV range in the insulator for hole doping and around 1 to 2 eV range for electron doping (Fig.2). This is clear evidence that even if doping introduces states in the middle of the gap (as argued based on ARPES measurements[17, 18]), changes in the electronic structure are further accompanied by direct melting (clear systematic changes in the leading-edge behavior) of the Mott gap in a momentum dependent manner. The observed low-energy continuum in the doped system is due to pair excitations involving quasiparticle-quasihole states that appear in the middle of the gap upon doping. In ARPES, only single electron state components of this continuum are seen as low-energy quasiparticle states[14]. The spectral distribution of the continuum is momentum dependent - changes upon doping are weak near the zone boundary ($q \sim (\pi, 0)$) as opposed to the zone center ($q \sim (2\pi, 0)$) (Fig.2). Fermi surface evolves asymmetrically by electron vs. hole doping and the differences in the detail momentum dependence of Mott gap melting in electron vs. hole doping would then be related to different topologies of Fermi surfaces in LSCO and NCCO as observed in ARPES. Quantitative analysis of the lower energy continuum weight below 0.8 eV is difficult due to the large quasielastic tails from structural diffuse scattering.

We focus rather on the spectral-edge behavior of the charge gap since low-energy weight is generated at the expense of the weight near the gap (Fig.2) and provides a connection or correlation (related to the spectral weight transfer) to the low-energy physics of these systems. A closer look at the gap in doped systems is interesting in its own right since a hierarchy of increasingly higher energy scales seems to be an emergent theme in the physics of doped Mott insulators[4]-[6]. Our results show that a gap feature similar to the undoped insulator exists at all doping and its dispersion is a remnant behavior from the insulator at all momenta as seen from Fig.1 and 2. We refer to this feature in the doped system as the Mott pseudogap or remnant Mott gap. A remnant Fermi surface-like behavior of single-particle spectral weight, $n(k)$, is observed in the undoped Mott insulator in ARPES studies by integrating within an energy window to include the occupied band [19]. In inelastic x-ray spectrum both occupied and unoccupied bands contribute hence our observation of remnant Mott gap in the doped system with similar momentum dispersion as in the insulator is consistent with a remnant Fermi surface (momentum behavior) behavior.

In an energy-loss experiment one measures particle-hole pair modes in metals and insulators and damped

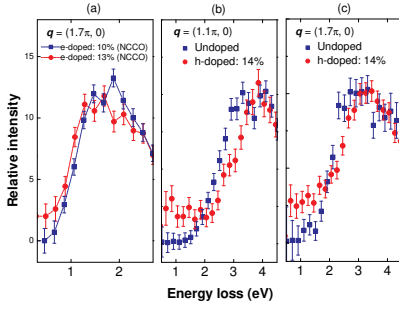


FIG. 2: Doping dependence of low-energy spectral weight with momenta near zone boundary for electron doping (left) and near zone center (middle) and near zone boundary (right) for hole doping.

plasmon modes in metals. The dynamics and nature of particle-hole pair ("excitons") in Mott insulators is less understood. The difficulty in describing the pair dynamics in a Mott insulator arises because of the fact that where as in a band insulator, excitons form via Coulomb interaction and the gap is due to Pauli exclusion, in Mott insulators the gap itself has a direct Coulombic origin[20]-[26]. However, this provides a possible connection between the particle-hole pair spectrum in doped Mott insulators to the charge-gap of the undoped insulator. When these insulators are doped eventually a weak Drude response emerges[8, 9] with corresponding plasma resonances being typically well below 1 eV making it difficult to observe in resonant x-ray experiments.

Fig.3(a) shows the energy vs. momentum behavior of the excitations edges for both *e*-doped and *h*-doped systems. We determine the leading-edge mid-point by taking a derivative of the energy-loss spectra with respect to the energy-loss axis. Undoped insulator shows the largest amount of dispersion which is about 500 meV. Upon hole doping dispersion seems to flatten out in a systematic manner. For the 3% *h*-doping (insulator) dispersion is reduced and follows a qualitative trend as seen in the undoped insulator. In the 14% *h*-doped sample dispersion is much reduced - it has flattened out quite a bit and is on the order of 100-150 meV. We also note that for all dopings, excitation-edge seem to be roughly pinned at the zone boundary $q \sim (\pi, 0)$ (Fig.3a).

Based on simple electronic structure considerations, doping of a few holes into two dimensional insulating cuprates creates a Zhang-Rice singlet state whose wavefunction is spread over four neighboring oxygen atoms whereas the doping of electron creates states in the upper Hubbard band whose character (wavefunction) is much more *d*-like with strongly localized character[20]-[23]. However, the way these states evolve to the high doping case is not well understood. Numerical finite-lattice simulations suggest asymmetric evolution of electron-hole pair modes in doped Mott insulators[22]. Our results suggest a broad agreement with such simulations. How-

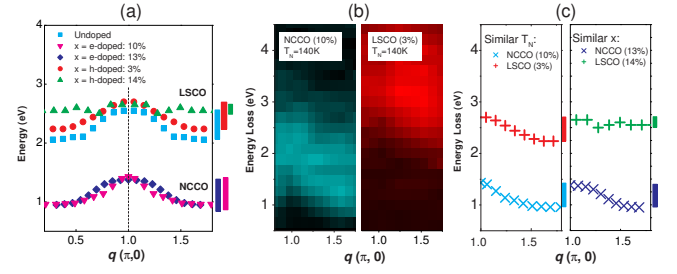


FIG. 3: Pair Bandwidth and Magnetism : (a) Energy vs. momentum relation of the leading-edge of the Mott gap determined by taking first derivatives of the image plots in Fig.1. Vertical bars outside the panel give a measure of the bandwidth.(b) Comparison of excitation spectra with different doping but same Neel temperature. (c) Comparison of pair dispersion for samples with same Neel temperature (left) and for samples with same doping but different Neel temperature (right) on either side of the phase diagram.

ever, a detailed comparison with lattice simulations are difficult since finite size of the lattice allows for only a few points to be studied. Much dramatic changes due to hole doping may be understood by combining ARPES results and Hubbard model spectral functions for electron-hole pair excitations. As evident from Fig.3(a), dispersion of pair excitations is weak from the zone center to about the half-way ($1.5\pi, 0$) to the zone boundary. In comparison with lattice simulations this effect has been argued to be due to the fact that the lowest energy state of the upper Hubbard band is near $(\pi, 0)$ as opposed to the momentum of $(\pi/2, \pi/2)$ of the top-most state of the lower Hubbard band[12, 22, 23]. Under this scenario, the x-ray spectra in lightly doped NCCO should not be much different from the undoped insulator since in the electron doped system lowest-energy excited electrons are in the upper Hubbard band and have very similar momenta as in the undoped insulator whereas in LSCO the lowest energy excited electrons are still in the lower (Zhang-Rice) Hubbard band. In other words, in case of hole doping, upper Hubbard band is not involved in creating the low energy electron-hole pair excitations hence the pair dynamics involves states of very different characters.

Fig.3(b) and (c) show a comparison of charge excitation response in 3%-LSCO and 10%-NCCO. Doping levels are picked so that both compounds have about the same Neel temperature ($\sim 140K$). Fig.3(b) shows the dispersion behavior of the leading-edge. Apart from an off-set in the energy scale (electron doped system has a smaller optical gap ~ 1.1 eV[9]) both compounds exhibit qualitatively similar momentum behavior and have the same amount of energy dispersion or pair bandwidth (~ 300 meV). This is on the order of $2J$ to $3J$ (where J is the exchange constant measured by neutron scattering (27)) which is a relevant magnetic energy scale for these systems. Fig.3(c) shows a comparison of LSCO(14%) and NCCO(13%) which have very similar doping levels. In

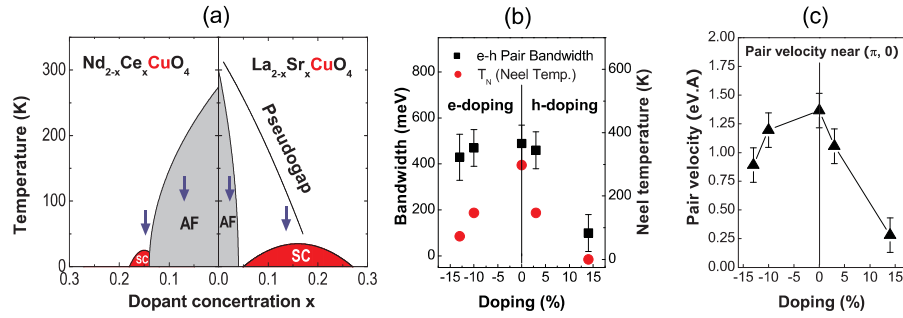


FIG. 4: Neel Order, Pair Bandwidth and Zone-Edge Velocity: (a). Electronic phase diagram of doped copper oxides. (b). Doping dependence of electron-hole pair bandwidth and Neel temperature. (c). Doping dependence of zone boundary $(\pi, 0)$ pair velocity.

the case of electron-doping (NCCO), the dispersive edge is much robust whereas a similar amount of hole doping leads to much **more** renormalization of the dispersion. Even for the 13% electron doped metallic NCCO dispersion remains on the order of 300 meV. This is a factor of two larger than the dispersion seen in the optimal hole doping. This is an indication of the dominance of anti-ferromagnetic correlations in NCCO which is consistent with findings in neutron studies of NCCO[28].

We look for possible direct correlation of electron-hole pair bandwidth measured in x-ray scattering and the Neel temperature which is the energy scale for the onset of long-range antiferromagnetic order in these systems. The cuprate phase diagram is shown in Fig.4(a). Fig.4(b) plots the pair bandwidth and Neel temperature as a function of doping. This correlation suggests that pair bandwidth decreases as long-range magnetic correlations decrease with doping. However, the collapse of bandwidth is much faster with hole doping than it is for electron doping. For the hole doping, pair bandwidth shows a direct scaling with Neel temperature which suggests a direct correlation with antiferromagnetic order in the hole doped systems. In case of electron doping bandwidth suppression with doping is weaker and weakly correlated with the doping fall-off of antiferromagnetic order. Robustness of strong short-range antiferromagnetic order is clearly seen in neutron scattering studies of highly doped NCCO systems[28]. We further introduce a velocity : the derivative of the excitation band near $(\pi, 0)$ which can be thought of as the zone-boundary pair velocity $(\delta\omega/\delta q)$. Such velocity exhibits similar correlation with doping. Like bandwidth, pair velocity is also highly asymmetric in electron vs. hole doping (Fig.4c). These results taken together, suggest that coherent propagation of electron-hole pairs are largely affected by the effective magnetic coupling or interaction strengths and reflects a strong electron-hole doping asymmetry in the electron dynamics of cuprates.

Our results reveal momentum structure of remnant Mott gap and electron-hole pair excitations in doped cuprates and their correlation with the phase diagram for

the first time (Fig.4). Although much theoretical efforts are needed to understand these observations we report here, results by themselves shed new light on the theories that argue for an intimate connection between the pseudogap and Mott charge gap and the importance of magnetic coupling strength in describing correlated electron behavior in cuprates[3, 29].

We acknowledge M. Beno, D. Casa and T. Gog for technical help. The experiments were performed at the Adv. Photon Source of Argonne National Lab which is supported by the U.S. Dept. of Energy, BES under Contract No. W-31-109-ENG-38. This work was partially supported by an NSF (DMR-0213706) grant. MZH acknowledges partial support through R.H. Dicke research award.

* To whom correspondence should be addressed: mzhazan@Princeton.edu

- [1] N. F. Mott, Proc. Phys. Soc. London A **62**, 416 (1949).
- [2] J. Hubbard, Proc. Roy. Soc. London A **277**, 237 (1964).
- [3] P. W. Anderson, Science **235**, 1196 (1987).
- [4] Y. Tokura, Physics Today **56**(7), 50 (2003).
- [5] V. J. Emery, S. A. Kivelson, Nature **374**, 434 (1995).
- [6] M. Imada et.al., Rev. Mod. Phys. **70**, 1039 (1998).
- [7] J. Orenstein, A. J. Millis, Science **288**, 468 (2000).
- [8] S. Uchida et.al., Phys. Rev. B **43**, 7942 (1991).
- [9] Y. Tokura et.al., Phys. Rev. B **41**, 11657 (1990).
- [10] P. M. Platzman, E. Isaacs Phys. Rev. B **57**, 11107 (1998).
- [11] C. C. Kao et al., Phys. Rev. B **54**, 16361 (1996).
- [12] M. Z. Hasan et.al., Science **288**, 1811 (2000).
- [13] M. Z. Hasan et.al., J. Elect. Spect. & Rel. Phen. **114**, 705 (2001).
- [14] P. Abbamonte et.al., Phys. Rev. Lett. **83**, 860 (1999).
- [15] Y.J. Kim et.al., Phys. Rev. Lett. **89**, 177003 (2002)
- [16] Y.J. Kim et.al., cond-mat/0404479 (2004).
- [17] A. Ino et.al., Phys. Rev. B **62**, 4137 (2000).
- [18] N.P. Armitage et.al., Phys. Rev. Lett. **87**, 147003 (2001).
- [19] F. Ronning et.al., Science **282**, 2067 (1998).
- [20] F.C. Zhang and K.K. Ng Phys. Rev. B **58**, 13520 (1998).
- [21] F.C. Zhang and T. M. Rice Phys. Rev. B **37**, 3759 (1988).
- [22] K. Tsutsui, T. Tohyama and S. Maekawa Phys. Rev.

- Lett. **91**, 117001 (2003).
- [23] K. Tsutsui, T. Tohyama and S. Maekawa Phys. Rev. Lett. **83**, 3705 (1999).
- [24] P. Wrobel and R. Eder, Phys.Rev. B **66**, 035111 (2002).
- [25] C. Kusko et.al., Phys. Rev. B **66**, 140513 (2002).
- [26] T. P. Devereaux et.al., Phys. Rev. Lett. **90**, 067402 (2003).
- [27] G. Aeppli et.al., Phys. Rev. Lett. **62**, 2052 (1989).
- [28] K. Yamada et.al., Phys. Rev. Lett. **90**, 137004 (2003).
- [29] R.B. Laughlin, Phys. Rev. Lett. **79**, 1726 (1997).